

See discussions, stats, and author profiles for this publication at: <https://www.researchgate.net/publication/239940604>

# Singlet Oxygen Generation by the Genetically Encoded Tag miniSOG

ARTICLE in JOURNAL OF THE AMERICAN CHEMICAL SOCIETY · JUNE 2013

Impact Factor: 12.11 · DOI: 10.1021/ja4020524 · Source: PubMed

CITATIONS

26

READS

77

6 AUTHORS, INCLUDING:



[Rubén Ruiz-González](#)

Universitat Ramon Llull

16 PUBLICATIONS 132 CITATIONS

[SEE PROFILE](#)



[Aitziber L Cortajarena](#)

Madrid Institute for Advanced Studies

52 PUBLICATIONS 766 CITATIONS

[SEE PROFILE](#)



[Montserrat Agut](#)

Universitat Ramon Llull

69 PUBLICATIONS 586 CITATIONS

[SEE PROFILE](#)



[Santi Nonell](#)

Universitat Ramon Llull

175 PUBLICATIONS 2,701 CITATIONS

[SEE PROFILE](#)

## Singlet Oxygen Generation by the Genetically Encoded Tag miniSOG

Rubén Ruiz-González,<sup>†</sup> Aitziber L. Cortajarena,<sup>‡,§</sup> Sara H. Mejias,<sup>‡,§</sup> Montserrat Agut,<sup>†</sup> Santi Nonell,<sup>\*,†</sup> and Cristina Flors<sup>\*,‡</sup><sup>†</sup>Institut Químic de Sarrià, Universitat Ramon Llull, Via Augusta 390, E-08017, Barcelona, Spain<sup>‡</sup>IMDEA Nanociencia, C/Faraday 9, Ciudad Universitaria de Cantoblanco, 28049 Madrid, Spain<sup>§</sup>CNB-CSIC-IMDEA Nanociencia Associated Unit "Unidad de Nanobiotechnología", Ciudad Universitaria de Cantoblanco, 28049 Madrid, Spain

## S Supporting Information

**ABSTRACT:** The genetically encodable fluorescent tag miniSOG is expected to revolutionize correlative light- and electron microscopy due to its ability to produce singlet oxygen upon light irradiation. The quantum yield of this process was reported as  $\Phi_{\Delta} = 0.47 \pm 0.05$ , as derived from miniSOG's ability to photooxidize the fluorescent probe anthracene dipropionic acid (ADPA). In this report, a significantly smaller value of  $\Phi_{\Delta} = 0.03 \pm 0.01$  is obtained by two methods: direct measurement of its phosphorescence at 1275 nm and chemical trapping using uric acid as an alternative probe. We present insight into the photochemistry of miniSOG and ascertain the reasons for the discrepancy in  $\Phi_{\Delta}$  values. We find that miniSOG oxidizes ADPA by both singlet oxygen-dependent and -independent processes. We also find that cumulative irradiation of miniSOG increases its  $\Phi_{\Delta}$  value  $\sim 10$ -fold due to a photoinduced transformation of the protein. This may be the reason why miniSOG outperforms other fluorescent proteins reported to date as singlet oxygen generators.

Genetically encodable fluorescent tags that are able to generate reactive oxygen species (ROS) have long been pursued as tools for microscopy. Specifically, fluorescent proteins (FPs) that generate singlet oxygen ( $^1\text{O}_2$ ) are of special interest for correlative light- and electron microscopy (EM).<sup>1</sup>  $^1\text{O}_2$  is produced when a photosensitizer (PS, in this case the fluorescent tag) is excited by light and transfers its excitation energy to molecular dioxygen.<sup>2</sup>  $^1\text{O}_2$  is highly reactive and photooxidizes substrates such as proteins, lipids, and nucleic acids which is relevant for photodynamic therapy (PDT) and chromophore-assisted laser inactivation (CALI).<sup>3</sup> For EM, these properties of  $^1\text{O}_2$  can be harnessed to locally transform diaminobenzidine (DAB) into an osmiophilic precipitate that can be imaged at high resolution within cells.<sup>4</sup> Although this reaction can also be initiated by a genetically encoded peroxidase and hydrogen peroxide,<sup>5</sup> there are advantages to DAB photooxidation by  $^1\text{O}_2$ , e.g. the short lifetime and diffusion length of  $^1\text{O}_2$  may result in an improved spatial resolution.<sup>4</sup>

Previously, we showed that variants from the green fluorescent protein (GFP) family can photosensitize  $^1\text{O}_2$ , although with low efficiency.<sup>7–9</sup> For example, TagRFP

photosensitizes  $^1\text{O}_2$  with a quantum yield ( $\Phi_{\Delta}$ ) of 0.004,<sup>9</sup> similar to that of the free GFP chromophore.<sup>7</sup> Although the value is sufficient and TagRFP has been successfully used for mechanistic studies in antimicrobial PDT,<sup>10</sup> FPs with higher  $\Phi_{\Delta}$  values are required. The photosensitizing protein KillerRed,<sup>11</sup> initially thought to produce  $^1\text{O}_2$ , is now known to produce other ROS.<sup>12,13</sup>

Recent efforts to produce genetically encodable tags that generate  $^1\text{O}_2$  have turned to engineering flavin mononucleotide (FMN)-binding FPs, since FMN is an efficient  $^1\text{O}_2$  photosensitizer ( $\Phi_{\Delta} = 0.51$ ).<sup>14</sup> MiniSOG (for "mini Singlet Oxygen Generator") is a 106 amino acid flavoprotein derived from phototropin 2.<sup>6</sup> Its small size (less than half that of GFP) is advantageous in protein fusions. Upon blue-light irradiation, miniSOG produces enough  $^1\text{O}_2$  to induce DAB photooxidation and also photoinduces cell ablation of neurons in *C. elegans*,<sup>15</sup> making it a potentially useful tool for CALI, PDT and optogenetics.

The  $^1\text{O}_2$  photosensitization efficiency of miniSOG had been reported as  $\Phi_{\Delta} = 0.47 \pm 0.05$ , basically equal to that of free FMN.<sup>6</sup> Because this value was found by an indirect chemical trapping method, we examined the kinetics of  $^1\text{O}_2$  formation and decay by directly monitoring its time-resolved NIR phosphorescence at 1275 nm and rationalized our observations by several complementary experiments that allowed us to conclude that the  $\Phi_{\Delta}$  value is much lower than previously reported.

The absorption and fluorescence spectra of purified miniSOG in PBS pH 7.4 are slightly blue-shifted relative to those of FMN and show more vibronic structure (Figure 1), indicating that the chromophore is tightly bound and confined to the protein active pocket.<sup>6,16</sup> The fluorescence of miniSOG shows features distinct from those of FMN, i.e. a lifetime of 5.1 ns vs 4.3 ns (Figure 1, inset) and a fluorescence quantum yield ( $\Phi_F$ ) of 0.37<sup>6</sup> vs 0.22,<sup>17</sup> respectively.

We used nanosecond laser flash photolysis to investigate the triplet state of miniSOG. Upon excitation of oxygen-free solutions at 355 nm, a transient signal with lifetime of 35  $\mu\text{s}$  was observed at 300 and at 700 nm (Figure S1a,b in Supporting Information [SI]), with a decay rate that was accelerated by oxygen (3  $\mu\text{s}$  in aerated solutions; Figure S1c in SI). This transient signal is ascribed to the triplet state of miniSOG. For

Received: February 26, 2013

Published: June 19, 2013



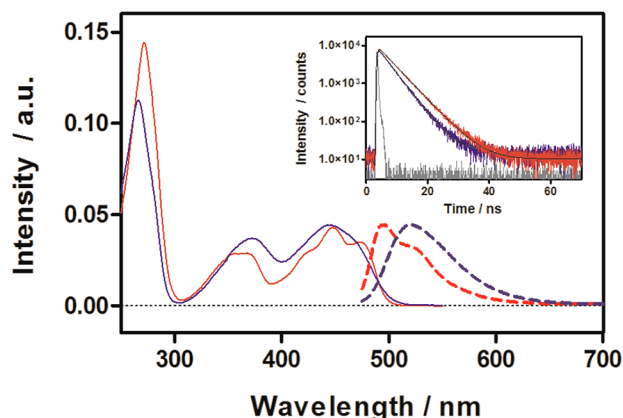


**Figure 1.** Basic photophysics of FMN (blue) and miniSOG (red) in solution. Absorption spectra (solid lines) and normalized fluorescence spectra (dashed lines).  $\lambda_{\text{exc}} = 450$  nm. (Inset) Time-resolved fluorescence decays at 500 nm and instrument response function (gray) upon excitation at 375 nm.

comparison, the triplet lifetime of FMN is 42  $\mu\text{s}$ , and the transient absorbance is 2-fold larger for an optically matched solution (Figure S1a,b in SI).

The most novel aspect of miniSOG is its greater photosensitization ability compared to those of FPs from the GFP family.<sup>6</sup> We confirmed this superior ability by studying the photoinduced cell death of *E. coli* bacteria expressing miniSOG and TagRFP<sup>10</sup>. Consistent with our expectations, miniSOG clearly outperformed TagRFP (Figure S2 in SI).

The greater photosensitization ability of miniSOG was explained by its apparently higher  $\Phi_{\Delta}$  value,  $0.47 \pm 0.05$ ,<sup>6</sup> very close to that of free FMN in solution ( $\Phi_{\Delta} = 0.51$ ).<sup>14</sup> We were therefore surprised to observe that the  $^1\text{O}_2$  phosphorescence signal at 1275 nm produced by miniSOG was much lower than that arising from an optically matched solution of FMN at the same excitation wavelength (Figure 2). Comparison of the intensity of miniSOG's  $^1\text{O}_2$  signal with that of optically matched reference solutions of FMN and phenalenone-2-sulfonate (PNS;  $\Phi_{\Delta} = 1$ ),<sup>18</sup> at the excitation wavelength of 355 nm and in the same solvent,<sup>19</sup> yielded  $\Phi_{\Delta} = 0.03 \pm 0.01$ , irrespective of solvent deuteration. For these studies, miniSOG was dissolved at a concentration of 2.5  $\mu\text{M}$  in either PBS or in a mixture of deuterated PBS and PBS (9:1) (hereafter dPBS) since deuteration increases the singlet oxygen lifetime and thus facilitates its detection.<sup>2</sup>

The  $\Phi_{\Delta}$  value reported for miniSOG was arrived at by using anthracene-9,10-dipropionic acid (ADPA) as a  $^1\text{O}_2$  probe.<sup>6</sup>  $\Phi_{\Delta}$  was determined by comparing the rates of ADPA photooxidation sensitized by miniSOG and by the reference FMN, the loss of ADPA being monitored by fluorescence. It was found that the rates of ADPA photooxidation were very similar, a result that we have reproduced in our laboratory. Surprisingly, when we repeated the experiment in dPBS, the ratio of photooxidation rates decreased to  $\sim 1/3$ , corresponding to an apparent  $\Phi_{\Delta}$  value of  $\sim 0.18$ . This lower value is totally unexpected if ADPA photooxidation occurs exclusively through a  $^1\text{O}_2$  reaction (as the longer  $^1\text{O}_2$  lifetime in dPBS would increase the rate of ADPA photooxidation, see discussion in SI)<sup>20</sup> and suggests that a more complex mechanism is involved.

To resolve the discrepancy between the  $\Phi_{\Delta}$  values measured by ADPA photooxidation and  $^1\text{O}_2$  phosphorescence, we used uric acid (UA), a different  $^1\text{O}_2$  chemical trap that reacts with

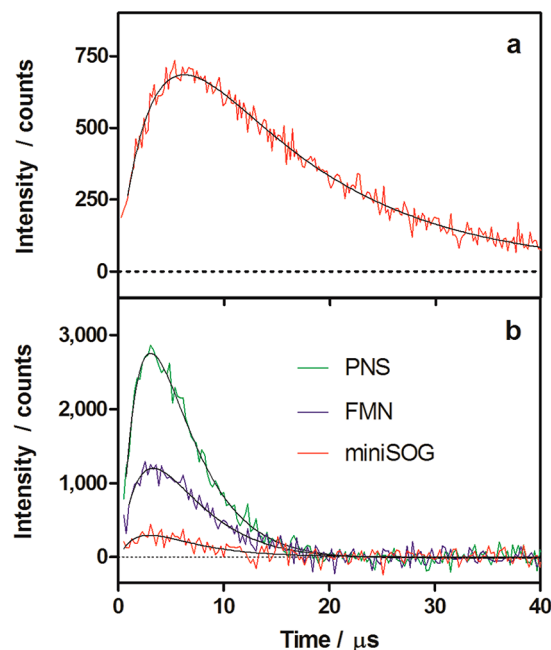


**Figure 2.** MiniSOG-photosensitized  $^1\text{O}_2$  formation. (a) Time-resolved  $^1\text{O}_2$  phosphorescence at 1275 nm of miniSOG in dPBS upon pulsed-laser irradiation at 355 nm. (b)  $^1\text{O}_2$  phosphorescence signals for optically matched solutions of the reference photosensitizer PNS (top, green line), FMN (middle, blue line), and miniSOG (bottom, red line) excited at 355 nm in PBS; intensities are proportional to  $\Phi_{\Delta}$  values.

$^1\text{O}_2$  through a mechanism different from that of ADPA.<sup>21,22</sup> With UA we obtained  $\Phi_{\Delta} = 0.03 \pm 0.01$  both in PBS and in dPBS upon excitation at 450 nm (Figure S3 in SI), equal to the value measured by time-resolved  $^1\text{O}_2$  phosphorescence (Table 1).

**Table 1.** MiniSOG's  $\Phi_{\Delta}$  Values Obtained by Different Techniques

method	$\Phi_{\Delta}$	
	PBS	dPBS
$^1\text{O}_2$ phosphorescence	$0.03 \pm 0.01$	$0.03 \pm 0.01$
uric acid	$0.03 \pm 0.01$	$0.03 \pm 0.01$
ADPA	$0.42 \pm 0.02$	$0.18 \pm 0.02$

In view of the results above, we concluded that processes other than reaction with  $^1\text{O}_2$  contributed significantly to ADPA photooxidation by miniSOG. While a full elucidation of such processes is beyond the scope of this communication, some attempts to clarify them were carried out. Photooxidation reactions may occur through two mechanisms: type-I, where the PS reacts directly with the substrate; or type-II, where  $^1\text{O}_2$  is formed instead.<sup>23</sup> Indeed, it has been reported that, in addition to their reaction with  $^1\text{O}_2$ , anthracenes can be oxidized by electron-transfer processes.<sup>24</sup> We have tested to see if that is the case for ADPA by studying its photooxidation by the electron-transfer photosensitizer 4-diphenyl-6-(4'-methoxyphenyl)pyrylium tetrafluoroborate, which acts as an electron acceptor and does not generate  $^1\text{O}_2$ .<sup>25</sup> Figures S4–S6 and discussion in the SI suggest that direct photoinduced electron transfer reactions contributing to ADPA photooxidation are plausible. It is also well-known that flavins are able to undergo electron transfer reactions with suitable electron donors.<sup>26,27</sup>

Thus, in addition to generating  $^1\text{O}_2$ , miniSOG may be capable of photooxidizing substrates by type-I mechanisms as well, which should be taken into account by researchers using miniSOG as a genetically encodable  $^1\text{O}_2$  source.

Our observations reveal a strong effect of the protein environment on miniSOG's  $^1\text{O}_2$  photosensitization efficiency. To better assess this, miniSOG was denatured in a 6 M solution of guanidinium hydrochloride (Gdn HCl)<sup>28</sup> (Figure S7 in SI). The efficiency of  $^1\text{O}_2$  photosensitization increased >10-fold upon protein denaturation (Figure 3b), coming close to the value for free FMN. This result highlights the effect of protein

residues, which can either modulate the excited states of FMN in the folded protein (and therefore affect the quantum yield of  $^1\text{O}_2$  production) or quench a fraction of  $^1\text{O}_2$  molecules before they can diffuse into the bulk medium.

It is well established that the photosensitized production of  $^1\text{O}_2$  occurs in three steps, each with its own efficiency: (1) PS's triplet state must be populated by intersystem crossing from the originally photoexcited singlet excited state; (2) triplet state molecules must be trapped by oxygen before they decay; (3) energy transfer from the triplet sensitizer to oxygen must take place.<sup>19</sup> Regarding the first process, it has been reported that the protein environment can modulate intersystem crossing in flavoproteins by electrostatic effects.<sup>16</sup> Consistent with this, we observe triplet transient absorbance signals for miniSOG that are smaller than those for free FMN (Figure S1a,b in SI) and a higher fluorescence quantum yield. Intersystem crossing in miniSOG would therefore be less efficient than in free FMN, although this effect alone fails to account for the 15-fold decrease in  $\Phi_\Delta$ . The triplet lifetime data likewise indicate that oxygen trapping of miniSOG's triplet state is almost as efficient as for FMN in water, which also rules out the second process as an important factor.

Our data thus suggest that  $^1\text{O}_2$  production by the flavin inside the protein is probably not much different than in the bulk aqueous solution. Even though FMN is located at about 10–15 Å from the protein surface, the triplet lifetime of miniSOG, similar to that of FMN, indicates that the chromophore is accessible to oxygen. Therefore, the most relevant cause for the difference in measured  $\Phi_\Delta$  may be attributed to a substantial fraction of the nascent  $^1\text{O}_2$  molecules being quenched on their way off the protein.<sup>29,30</sup> This notion is supported by the fact that miniSOG contains a large number of amino acids that are effective  $^1\text{O}_2$  quenchers: tryptophan (Trp;  $\times 1$ ), histidine (His;  $\times 1$ ), tyrosine (Tyr;  $\times 3$ ), and methionine (Met;  $\times 2$ ) (Figure 3a), plus the His-tag ( $\times 6$ ) used for purification. Experimental support was obtained from measurements of  $^1\text{O}_2$  upon cumulative irradiation of miniSOG. As shown in Figure 3c the amplitude of the  $^1\text{O}_2$  phosphorescence signal, and therefore the  $\Phi_\Delta$  value, increased  $\sim 10$ -fold after irradiation (taking into account the small absorbance decrease upon irradiation, Figure S8a in SI). Two reasons may account for this observation: the progressive photoinactivation of the amino acids responsible for  $^1\text{O}_2$  quenching or the buildup of FMN photoproducts. Photolysis of free FMN leads to a decrease in the  $^1\text{O}_2$  phosphorescence signal (Figure S9 in SI), suggesting that the photoinactivation of quenching residues is the most plausible explanation. Absorption and fluorescence measurements rule out any contribution of protein denaturation to this effect (Figure S8a,b in SI). On the other hand, removal of the His-tag did not change the  $\Phi_\Delta$  value, consistent with this tag being far away from the site of  $^1\text{O}_2$  production. This is relevant for drawing comparisons between miniSOG's photochemistry as a purified protein in solution and as a fusion partner in a cell.

Finally, note that redox-active amino acids (Trp, Tyr) that are involved in electron transfer reactions in some flavoproteins are also present in miniSOG's sequence,<sup>31–33</sup> but these residues are not in the chromophore vicinity (Figure 3a) and are not likely to participate in direct electron transfer reactions with FMN (see ref 34 and refs therein). For example, Trp81Phe mutation does not improve  $^1\text{O}_2$  photosensitization ( $\Phi_\Delta = 0.01$ ), which seems to rule out the direct participation of this residue in electron transfer reactions.

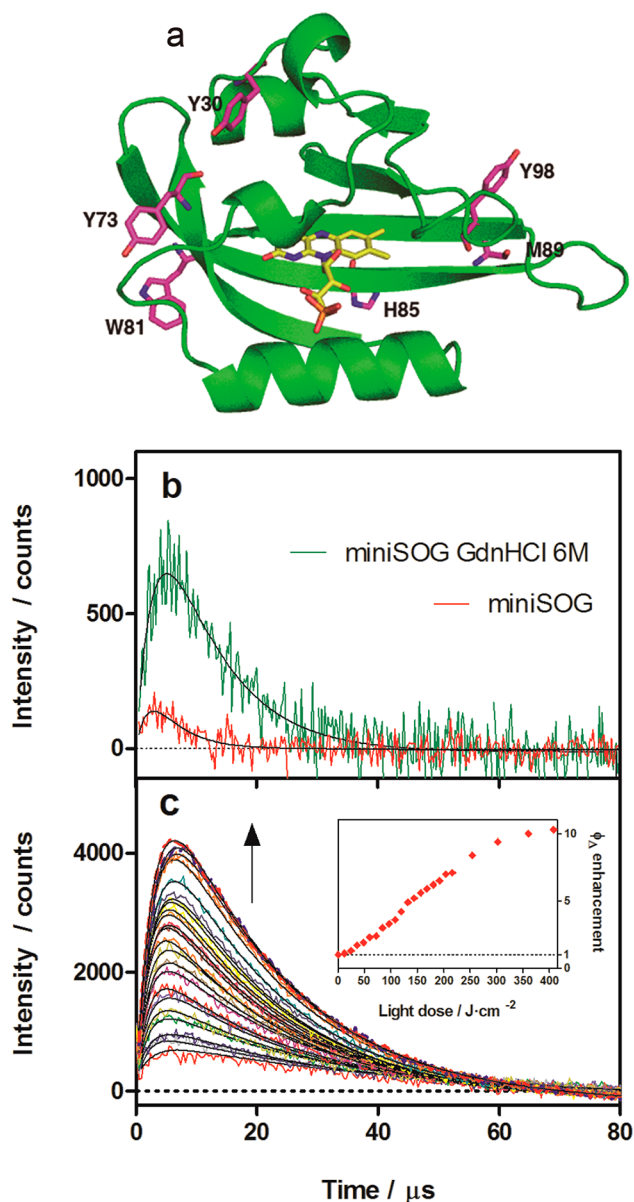


**Figure 3.** (a) MiniSOG's molecular model based on the structure of iLOV protein (PBD ID: 4eet), built using the Swiss-model server (<http://swissmodel.expasy.org/>). The backbone of miniSOG is shown as a green ribbon, FMN as orange sticks, and the amino acids that may quench  $^1\text{O}_2$  as magenta sticks. (b) Time-resolved near-IR phosphorescence of  $^1\text{O}_2$  photosensitized by folded (red line) or denatured (green line) miniSOG in PBS. (c) Effect of cumulative irradiation of miniSOG on its  $^1\text{O}_2$  photosensitization ability in dPBS.  $\lambda_{\text{exc}} = 355$  nm;  $\lambda_{\text{obs}} = 1275$  nm. (Inset)  $\Phi_\Delta$  enhancement.



In summary, we have unravelled the photochemical behavior of the miniSOG FP using a range of spectroscopic techniques. Our most important result is the revision of the  $\Phi_{\Delta}$  value that we determined to be  $0.03 \pm 0.01$ , ~15-fold lower than reported previously.<sup>6</sup> We have accounted for possible reasons for the discrepancy (e.g. the contribution of  $^1\text{O}_2$ -independent processes to ADPA oxidation), and we have discovered that miniSOG undergoes a photoinduced transformation that increases its  $\Phi_{\Delta}$  value by ~10-fold. This may prove advantageous for EM imaging and other potential uses of miniSOG. A recent communication in which miniSOG is shown to outperform ReAsH in EM experiments suggests that this may indeed be the case.<sup>35</sup> Finally, it is worth noting that the screening method used to develop miniSOG was based on evaluating the photobleaching of a fused fluorescent protein. Photobleaching can be due not only to  $^1\text{O}_2$  but also to other ROS and radical reactions. Thus, there is still opportunity to improve the value of  $\Phi_{\Delta}$  by screening with another, more specific method that selects for singlet oxygen-generating mutants. Detection of  $^1\text{O}_2$  phosphorescence at 1275 nm as described in this communication is thus ideally suited to develop new and better miniSOG variants.

## ■ ASSOCIATED CONTENT

### ■ Supporting Information

Discussion, further miniSOG photochemical characterization, ADPA photooxidation experiments,  $\Phi_{\Delta}$  calculations, effects upon denaturation, and microbiology experiments; description of the materials and procedures used in the study. This material is available free of charge via the Internet at <http://pubs.acs.org>.

## ■ AUTHOR INFORMATION

### Corresponding Author

cristina.flors@imdea.org; santi.nonell@iqs.url.edu

### Notes

The authors declare no competing financial interest.

## ■ ACKNOWLEDGMENTS

Financial support was obtained from the Spanish Ministerio de Economía y Competitividad (CTQ2010-20870-C03-01, S.N., and RYC-2011-07637, C.F.), the European Commission (IRG-246688, A.L.C. and Marie Curie COFUND “AMAROUT” Program, A.L.C. and C.F.). R.R.G. thanks the Generalitat de Catalunya (DURSI) and the European Social Fund for a predoctoral fellowship. S.H.M. thanks IMDEA-Nanociencia for a “Ayuda de Iniciación a la Investigación” fellowship. We are very grateful to Prof. Roger Tsien (UCSD, U.S.A.) for the gift of the miniSOG plasmid and to Dr. Xiaokun Shu (UCSF, U.S.A.) for helpful discussions.

## ■ REFERENCES

- (1) Smith, C. *Nature* **2012**, 492, 293–297.
- (2) Ogilby, P. R. *Chem. Soc. Rev.* **2010**, 39, 3181–3209.
- (3) McLean, M. A.; Rajfur, Z.; Chen, Z.; Humphrey, D.; Yang, B.; Sligar, S. G.; Jacobson, K. *Anal. Chem.* **2009**, 81, 1755–1761.
- (4) Deerinck, T. J.; Martone, M. E.; Lev-Ram, V.; Green, D. P.; Tsien, R. Y.; Spector, D. L.; Huang, S.; Ellisman, M. H. *J. Cell Biol.* **1994**, 126, 901–910.
- (5) Martell, J. D.; Deerinck, T. J.; Sancak, Y.; Poulos, T. L.; Mootha, V. K.; Sosinsky, G. E.; Ellisman, M. H.; Ting, A. Y. *Nat. Biotechnol.* **2012**, 30, 1143–1148.
- (6) Shu, X.; Lev-Ram, V.; Deerinck, T. J.; Qi, Y.; Ramko, E. B.; Davidson, M. W.; Jin, Y.; Ellisman, M. H.; Tsien, R. Y. *PLoS Biol.* **2011**, 9, e1001041.
- (7) Jiménez-Banzo, A.; Nonell, S.; Hofkens, J.; Flors, C. *Biophys. J.* **2008**, 94, 168–172.
- (8) Jiménez-Banzo, A.; Ragàs, X.; Abbruzzetti, S.; Viappiani, C.; Campanini, B.; Flors, C.; Nonell, S. *Photochem. Photobiol. Sci.* **2010**, 9, 1336–1341.
- (9) Ragàs, X.; Cooper, L. P.; White, J. H.; Nonell, S.; Flors, C. *ChemPhysChem* **2011**, 12, 161–165.
- (10) Ruiz-González, R.; White, J. H.; Agut, M.; Nonell, S.; Flors, C. *Photochem. Photobiol. Sci.* **2012**, 11, 1411–1413.
- (11) Bulina, M. E.; Chudakov, D. M.; Britanova, O. V.; Yanushevich, Y. G.; Staroverov, D. B.; Chepurnykh, T. V.; Merzlyak, E. M.; Shkrob, M. A.; Lukyanov, S.; Lukyanov, K. A. *Nat. Biotechnol.* **2006**, 24, 95–99.
- (12) Serebrovskaya, E. O.; Edelweiss, E. F.; Stremovskiy, O. A.; Lukyanov, K. A.; Chudakov, D. M.; Deyev, S. M. *Proc. Natl. Acad. Sci. U.S.A.* **2009**, 106, 9221–9225.
- (13) Vegh, R. B.; Solntsev, K. M.; Kuimova, M. K.; Cho, S.; Liang, Y.; Loo, B. L.; Tolbert, L. M.; Bommarius, A. S. *Chem. Commun.* **2011**, 47, 4887–4889.
- (14) Baier, J.; Maisch, T.; Maier, M.; Engel, E.; Landthaler, M.; Baumler, W. *Biophys. J.* **2006**, 91, 1452–1459.
- (15) Qi, Y. B.; Garren, E. J.; Shu, X.; Tsien, R. Y.; Jin, Y. *Proc. Natl. Acad. Sci. U.S.A.* **2012**, 109, 7499–7504.
- (16) Schüttrigkeit, T. A.; Kompa, C. K.; Salomon, M.; Rüdiger, W.; Michel-Beyerle, M. E. *Chem. Phys.* **2003**, 294, 501–508.
- (17) Valle, L.; Vieyra, F. E.; Borsarelli, C. D. *Photochem. Photobiol. Sci.* **2012**, 11, 1051–1061.
- (18) Nonell, S.; González, M.; Trull, F. R. *Afinidad* **1993**, 50, 445–450.
- (19) Nonell, S.; Braslavsky, S. E. *Methods Enzymol.* **2000**, 319, 37–49.
- (20) Foote, C. S.; Clennan, E. L. In *Active Oxygen in Chemistry*; Foote, C. S., Valentine, J. S., Greenberg, A., Liebman, J. L., Eds.; SEARCH series, Vol. 2; Blackie Academic and Professional: Glasgow, 1995; pp 105–140.
- (21) Matsuura, T.; Saito, I. *Tetrahedron* **1968**, 24, 6609–6614.
- (22) Rabello, B. R.; Gerola, A. P.; Pelloso, D. S.; Tessaro, A. L.; Aparicio, J. L.; Caetano, W.; Hioka, N. J. *Photochem. Photobiol., Sect. A* **2012**, 238, 53–62.
- (23) Foote, C. S. *Photochem. Photobiol.* **1991**, 54, 659–659.
- (24) Kotani, H.; Ohkubo, K.; Fukuzumi, S. *J. Am. Chem. Soc.* **2004**, 126, 15999–16006.
- (25) Miranda, M. A.; Garcia, H. *Chem. Rev.* **1994**, 94, 1063–1089.
- (26) Crovetto, L.; Braslavsky, S. E. *J. Phys. Chem. A* **2006**, 110, 7307–7315.
- (27) Barbieri, Y.; Massad, W. A.; Díaz, D. J.; Sanz, J.; Amat-Guerri, F.; García, N. A. *Chemosphere* **2008**, 73, 564–571.
- (28) Munro, A.; Noble, M. In *Flavoprotein Protocols*; Chapman, S. K., Reid, G. A., Eds.; Humana Press Inc.: Totowa, NJ; 1999; Vol. 131, pp 25–48.
- (29) Chin, K. K.; Trevithick-Sutton, C. C.; McCallum, J.; Jockusch, S.; Turro, N. J.; Scaiano, J. C.; Foote, C. S.; Garcia-Garibay, M. A. *J. Am. Chem. Soc.* **2008**, 130, 6912–6913.
- (30) Jensen, R. L.; Arnbjerg, J.; Ogilby, P. R. *J. Am. Chem. Soc.* **2012**, 134, 9820–9826.
- (31) Zhong, D.; Zewail, A. H. *Proc. Natl. Acad. Sci. U.S.A.* **2001**, 98, 11867–11872.
- (32) Mataga, N.; Chosrowjan, H.; Taniguchi, S.; Tanaka, F.; Kido, N.; Kitamura, M. *J. Phys. Chem. B* **2002**, 106, 8917–8920.
- (33) Kao, Y. T.; Tan, C.; Song, S. H.; Ozturk, N.; Li, J.; Wang, L.; Sancar, A.; Zhong, D. *J. Am. Chem. Soc.* **2008**, 130, 7695–7701.
- (34) Kao, Y. T.; Saxena, C.; He, T. F.; Guo, L.; Wang, L.; Sancar, A.; Zhong, D. *J. Am. Chem. Soc.* **2008**, 130, 13132–13139.
- (35) Boassa, D.; Berlanga, M. L.; Yang, M. A.; Terada, M.; Hu, J.; Bushong, E. A.; Hwang, M.; Masliah, E.; George, J. M.; Ellisman, M. H. *J. Neurosci.* **2013**, 33, 2605–2615.